Separated Flow Over a Body of Revolution

F. J. Marshall* and F. D. Deffenbaugh†
Purdue University, West Lafayette, Ind.

A method is developed to determine the flowfield of a body of revolution in separated flow. The technique employed is the use of the computer to integrate various solutions and solution properties of the sub-flowfields which make up the entire flowfield without resorting to a finite difference solution to the complete Navier-Stokes equations. The technique entails the use of the unsteady cross flow analogy and a new solution to the required two-dimensional unsteady separated flow problem based upon an unsteady discrete-vorticity wake. Data for the forces and moments on bodies of revolution at high angle of attack (outside the range of linear inviscid theories) such that the flow is substantially separated are produced which compare well with experimental data at low speeds. In addition, three-dimensional steady separation regions and wake vortex patterns are determined.

Nomenclature

$a(t)$ = radius as function of time
$\tilde{a}$ = characteristics length of two dimensional unsteady flowfield
C_D = coefficient of drag
$C_{M,\lambda}$ = coefficient of pitching moment about point $[0,0,\lambda\mathfrak{L}]$
c_n = coefficient of sectional normal force
C_N = coefficient of normal force
C_p = coefficient of pressure
d = maximum body diameter
D = drag
f = fineness ratio $(=\mathfrak{L}/d)$
$H(t)$ = step function $(=0, t\leq 0, =1, t>0)$
$\mathfrak{L}$ = body length
$\mathfrak{L}_\beta$ = distance of vrotex from origin $(=[x_\beta{}^2+y_\beta{}^2]^{1/2})$
m_k = location of vortex born from boundary layer
m_{rk} = location of vortex born from rear shear layer
M = pitching moment
N = normal force
p = pressure
q = dynamic pressure
r = polar radius
r_o = body radius
$r_\mathfrak{L}$ = vortex core radius
$\bar{r}$ = boundary-layer variable
∞ = outer flow evaluated at surface
i = inner flow
$\bar{}$ = inner flow
f = forward
r = rear

Subscripts

m = extremum
0 = stagnation point
s = separation point
k = at time t_k
β = point vortex β
∞ = freestream value
r,θ,t = partial derivatives

Miscellaneous

$\hat{}$ = three-dimensional steady flow (in contradistinction to two dimensional unsteady flow)
$\cdot$ $\equiv d()/dt$
$\Delta\theta,\Delta\bar{r},\Delta t_k =$ $t_{k+1}-t_k$ = numerical integration parameters
Re_{3DS} = Reynolds number, three dimensional steady $(=V\mathfrak{L}/\nu)$
Re_{2DUS} = Reynolds number, two dimensional unsteady $(=U\tilde{a}/\nu)$
t = time
S = frontal area
U = $V\sin\alpha$
V = freestream velocity
W = $V\cos\alpha$
$[\tilde{u},\tilde{v}]$ = Cartesian velocity components
$[u,v]$ = polar velocity components
$[x,y,z,t]$ = coordinates
α = angle of attack
Γ = circulation
δ = $1/(Re_{2DUS})^{1/2}$
θ = polar angle
λ = moment arm coefficient $(0\leq\lambda\leq 1)$
ν = kinematic viscosity
ρ = density
τ = wall shear stress
Φ = potential function
Ψ = stream function
ω = vorticity

Superscripts

$*$ = dimensional
$\circ$ = outer flow

Received April 18, 1974; revision received September 6, 1974. This work was partially supported by NASA Grant NGR15-005-119 and has been carried out in partial fulfillment of the requirements for the degree of Doctor of Philosophy in the School of Aeronautics and Astronautics, Purdue University. The authors are indebted to E. J. Landrum, NASA Langley Research Center, for her technical contributions.

Index categories: Aircraft Aerodynamics; Launch Vehicle and Missile Aerodynamics.

*Professor, School of Aeronautics and Astronautics, Member AIAA.

†Chrysler Fellow, School of Aeronautics and Astronautics.

Introduction

THE objective of the present work is to develop a numerical computation method to determine the flowfield of a body of revolution in steady, high Reynolds' number, *separated* flow (e.g., a body at high angle of attack), including the prediction of forces and moments. For flowfields in which separation must be taken into account, the assump-

tions of inviscid flow and linearized theory are invalid and the only general theoretical approach is to solve the Navier-Stokes equations in finite-difference form by means of a computer. However, this approach is not capable, to date, of dealing with such a complete problem. (In recent symposia[1,2] this problem is not treated). In this work it is intended to approach the problem of separated flow by a more phenomenological approach: the integration of known solutions and solution properties employing a computer without any a priori knowledge of the flowfield required.

Two particular techniques are employed. The first is the unsteady cross flow analogy (or viscous cross flow analogy or impulse flow analogy), which is based up the assunption of an equivalence between three-dimensional steady flow and two-dimensional unsteady flow. This assumption is a heuristic one based primarily upon experimental data. With this technique, the three-dimensional steady separated flow problem is reduced to a two-dimensional unsteady separated flow problem. The second technique, applicable to the latter problem, is based upon the assumption that the two dimensional unsteady wake can be described by a distribution of inviscid point vortices, originating from the separation of shear layers, superimposed on the unseparated potential flow solution, These point vortices are modified by diffusion.

This approach then entails the solutions to two distinct problems. The background and analysis for each are presented in the following two sections. The combined theory is then applied to bodies of revolution at angle of attack. Results for the normal force, pitching moment, separation regions, and vortex wake patterns are compared with experimental data.

Unsteady Cross Flow

The basic problem is to determine the flowfield and to predict the forces and moments on a three-dimensional body in a steady uniform flow at an angle of attack, α, of arbitrary magnitude such that the flow may be separated. The body shape is given by the radial distribution $r_0(\hat{z})$ over a length, $\mathcal{L}$. The freestream speed is $V$with components along and normal to the axis of symmetry, $W = V\cos\alpha$ and $U = V\sin\alpha$, respectively. The Reynolds' numbers $Re_{3DS} = V\mathcal{L}/\nu$. This problem is approached by using the unsteady cross flow analogy applied to a body of revolution. The essence of this technique is found in applying the (dimensional) transformation $[\hat{x}^*, \hat{y}^*, \hat{z}^*, t^*] = [x^*, y^*, z^* + Wt^*, t^*]$ and considering the flowfield in the plane $z^* = 0$ (see Fig. 1). In this plane, the flow field is that induced by a circular cylinder of time-varying radius (correlated with the thickness distribution of the body) in a uniform, viscous, incompressible freestream of velocity $U = V\sin\alpha$. Information available from the relatively simpler two-dimensional unsteady flow is thus applicable to the three-dimensional steady flowfield. In particular, the two-dimensional unsteady drag distribution with time is transformed to the longitudinal normal force distribution of the three-dimensional steady flowfield yielding the normal force and pitching moment on the given body at angle of attack.

While the unsteady cross-flow appears to be the only technique available for the determination of forces on three-dimensional bodies in separated flows, it must be viewed as quasi-empirical since there exists no general transformation between the two-dimensional unsteady and the three-dimensional steady Navier-Stokes equations (Ref. 3, p. 415 and Ref. 5, p. 464). From a theoretical point of view there exist unresolved questions since the use of the unsteady cross flow concept implies no upstream influence in the three-dimensional steady flowfield which does not hold in separated subsonic flow[5] nor in separated supersonic flow. [In the later case, hyperbolicity exists in the unseparated domain but not in the wake.] Its use also implies that a steady three-dimensional turbulent boundary layer is describable by a two-dimensional unsteady laminar or turbulent boundary layer with the corresponding separation regions correlated. The physics of

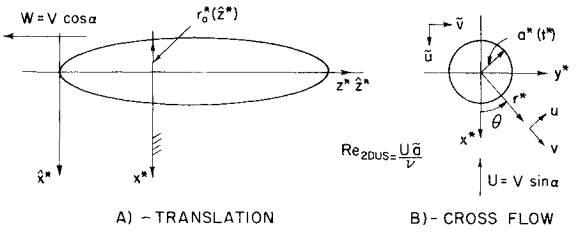

Fig. 1 Coordinate systems of transformation.

this point are obscure,[3] further complicated by the scale effect in experimental data.[6] In this work, following the objective of not requiring empirical input, two-dimensional unsteady laminar boundary layers have been used as indicated by the cross-flow Reynolds number of the test cases and the resulting separation region is carried over to the three-dimensional body by means of the transformations given next. Since the present program has only laminar boundary-layer capability, the method is confined to cross-flow Reynolds numbers $< 10^5$.

In this context then, it is not surprising that in past work employing the unsteady cross flow analogy,[7-17] the correlation between the three-dimensional steady and two-dimensional unsteady flow has been achieved in various ways, often requiring ad hoc experimental data. An early attempt at providing theoretical justification for the unsteady cross-flow analogy was made in Ref. 18 in which the boundary layer was treated rigorously. However, it was found that the difficulties involved in the separation region were dominant.

Transformations

The particular form of the unsteady cross-flow analogy used in the present work is given by the following geometry and force transformations between three-dimensional steady and two-dimensional unsteady flows. It is to be noted that these transformations are direct ones, assuming no further knowledge of the flowfields and requiring no empirical data.

Given the three-dimensional steady flowfield, the geometry transformation is obtained as follows: if a velocity $W = V\cos\alpha$ is superimposed on the steady three-dimensional flowfield, the flowfield of Fig. 1a results. Then if attention is confined to the plane $\hat{z}^* = 0$, an unsteady two-dimensional flowfield about a body whose radius changes with time with a constant velocity at infinity results. The goemetry transformation is then, in non-dimensional form,

$$a(t) = (d/2\tilde{a})\, r_0(\hat{z}),\ t = (df/\tilde{a})\,\hat{z}\tan\alpha$$

$$0 \le \hat{z} \le 1\ ;\ 0 \le t \le (df/\tilde{a})\tan\alpha \qquad (1)$$

where $r_0 = 2r_0^*/d$, $\hat{z} = \hat{z}^*/\mathcal{L}$, $t = Ut^*/\tilde{a} = t^*(V/\tilde{a})\sin\alpha$, $f = \mathcal{L}/d$ and $\tilde{a}$ an average radius in the two-dimensional unsteady problem.

The force transformation is given by equating the normal force distribution along the body, $dN/d\hat{z}^*$, to the drag induced in the two-dimensional unsteady flow problem, $D(t)$, with equal freestream conditions and employing the above geometry transformation. In non-dimensional form this is (with $\hat{p}^*_\infty = p^*_\infty$ and $\hat{\rho}^*_\infty = \rho^*_\infty$,

$$c_n(\hat{z}) = (2\tilde{a}/d)\sin^2\alpha C_D(t),\ Re_{3DS} = (fd/\tilde{a}\sin\alpha)Re_{2DUS} \qquad (2)$$

where

$$c_n(\hat{z}) = \frac{2dN/d\hat{z}^*}{\hat{\rho}V^2 d} \qquad (3)$$

$$C_D(t) = \frac{2D(t^*)}{\rho U^2(2\tilde{a})} = \frac{1}{2}\int_0^{2\pi} C_p\cos\theta\, a(t)d\theta + \frac{1}{2}\int_0^{2\pi} \tau\sin\theta\, a(t)d\theta \qquad (4)$$

in which $C_p = 2(2p^* - p^*_\infty)/\rho U^2$ and $\tau = 2\tau^*/\rho U^2$ the non-dimensional wall stress. This transformation ignores longitudinal shear stresses which for aerodynamic shapes (such that $f = \mathcal{L}/d >> 1$) should contribute little to normal forces and pitching moment.

With $C_D(t)$ available from the two-dimensional unsteady problem and $c_n(\hat{z})$ available from the above force transformation, the normal force and pitching moment about a point $[\bar{x},\bar{y},\bar{z}] = [0,0,\lambda]$ are obtained as follows:

$$C_N = (4f/\pi)\int_0^1 c_n(\hat{z})d\hat{z} \tag{5}$$

$$C_{M,\lambda} = (-4f/\pi)\int_0^1 [\hat{z} + (r_0/4f^2)$$

$$dr_0/d\hat{z}]c_n(\hat{z})d\hat{z} + \lambda C_N \tag{6}$$

such that $N = C_N\hat{\rho}V^2S/2$ and $M_\lambda = C_{M,\lambda}\hat{\rho}V^2S\mathcal{L}/2$ with frontal area S. Equations (5) and (6) are exact expressions for the normal force and pitching moment on an arbitrary body due to an arbitrary pressure distribution. (The inclusion of only cross-flow plane shear stresses would render them as approximations to equations with pressure and shear stresses but the contribution of cross-flow stresses to $C_D(t)$ in Eq. (3), and hence to $c_n(\hat{z})$ in Eq. (2), is negligible). The expression for the pitching moment coefficient includes moment arms along the $\hat{z}$ and $\hat{x}$ axes. The resulting c_n, C_N, and $C_{M,\lambda}$ are then compared with experimental data.

Two-Dimensional Unsteady Separated Flow

The problem is to find the flowfield induced by a circular cylinder of time-varying radius in a uniform stream of a viscous incompressible fluid (Fig. 1b). The flowfield is that of a uniform flow with no body present for $t<0$. At $t=0$ a circular body appears at the origin with a radius $a(t)$ such that $a(0)=0$. During the initial stages a boundary layer (assumed to be laminar) is formed on the circular cylinder. At later times the boundary layer separates from the cylinder, creating vorticity in the flowfield immediately past the cylinder of time-varying radius. Thus a wake is formed which corresponds to the lee-side separation of three-dimensional flow.

In previous work employing the unsteady cross flow with a body of revolution,[7-17] the two-dimensional unsteady solution was derived from a direct use of experimental data or the use of inviscid solutions with ad hoc experimental data to describe the viscous effects. Of note is the work of Ref. 11 which used the finite difference approach for the two-dimensional unsteady problem. These solutions are a generalization of the class of solutions arising from the problem of a body of constant radius impulsively started from rest, a classical problem in separated flow.[19] In these solutions the long-time behavior is of primary interest while for the use of the cross-flow analogy, the short-time behavior is required. For the constant-radius problem there are solutions to the finite difference Navier-Stokes equations[20] and purely inviscid solutions[9,10] requiring empiricism for separation phenomena.

The approach in the present work is to obtain a solution to the problem involving a time-varying radius cylinder which includes viscous effects (the primary mechanism being the separation of the unsteady boundary layer) without the need for empirical data nor resorting to a complete finite difference solution to the Navier-Stokes equation. The basic assumption is that the wake can be described by a distribution of inviscid point vortices born at shear layer separation points, superimposed on the potential flow and modified by diffusive effects. This assumption follows the physics of the time evolution of the wake. Such an approach can employ known potential solutions and known techniques for integration of boundary-layer equations interrelated by wake physics. The method is as follows: the solution at early times (sometimes referred to as the cone problem) will be approximated by the small time analytical solution (since numerical integration follows, an analytical solution is required for initial conditions) for a circular cylinder of constant radius impulsively started from rest in a viscous incompressible fluid.[21] The solutions for the laminar boundary layer on an expanding-contracting cylinder for later times are then obtained by numerical integration of the boundary-layer equations employing a modification of Hall's scheme.[22] With succeeding times, the boundary layer separates starting at the rear stagnation point and the point of separation moves upstream. At the point of separation, the vorticity flux across the boundary layer is found and during a time Δt, corresponding to the time of integration of the boundary layer, this flux is summed up and represented by a point vortex. This point vortex is convected downstream and its effect is modified by diffusion. Thus, the wake is formed of these point vortices superimposed on the original potential flow. The wake grows, being continually fed with vorticity by the separating boundary layer, while outside of the wake and the boundary layer, irrotational flow exists.

It is to be noted that the no-slip condition is satisfied on the portion of the cylinder covered by the boundary layer but not on the remaining portion. The wake model as depicted while reducing the surface speed of potential flow is not sufficient to yield a surface speed sufficiently less than freestream speed to approximate to a no-slip condition. Thus a shear layer on the rear of the cylinder, similar to a boundary layer but with a rotational outer flow will be introduced to satisfy the no-slip condition. This rear shear layer may separate, creating vorticity in the wake of the sign opposite to that shed by the boundary-layer separation.

With this approach the flowfield is decomposed into a set of sub-flowfields and their interactions. The governing equations and their solution are given in the following.

Outer Flow

The flow outside the boundary layer-rear shear layer is assumed to be the unsteady classical potential flow (uniform flow and source and double at origin) over a cylinder with time dependent radius plus the potential flow induced by a set of point vortices.

In terms of the non-dimensional quantities $[x,y,t] = [x^*/\tilde{a}, y^*/\tilde{a}, Ut^*/\tilde{a}]$, $r = r^*/\tilde{a}^*$, $\Phi + i\Psi = (\Phi^* + i\Psi^*)/U\tilde{a}$, $\omega = \tilde{a}\tilde{\omega}^*/U$, $\Gamma = \Gamma^*/U\tilde{a}$, the equations for the outer flow are

$$\text{DE } \Delta\Psi(x,y,t) = \omega(x,y,t)$$

$$\text{IC } t=0\ \Psi = y \tag{7}$$

$$\text{BC } 1) r = a(t): \Psi = -a\dot{a}\theta$$

$$2) r \to \infty: \Psi \to y$$

where $\omega(x,y,t) = \sum_\beta \Gamma_\beta \delta(x - x_\beta)\delta(y - y_\beta)$,

(δ being the delta function) such that

$$\iint \omega dS = \sum_\beta \Gamma_\beta.$$

The $\omega(x,y,t)$ arises from vorticity created by the separation of the boundary and rear shear layers.

The solution is

$$w = \Phi + i\Psi = z + \frac{a^2}{z} - a\dot{a}\log z +$$

$$i\sum_\beta \frac{\Gamma_\beta}{2\pi}\log\frac{(z - z_\beta)z}{(z - a^2 z_\beta/|z_\beta|^2)z_\beta} \tag{8}$$

where

$$z=x+iy=re^{i\theta}$$

$$z_\beta=x_\beta+iy_\beta=\mathfrak{L}_\beta e^{i\theta_\beta}$$

$$z-z_\beta=(x-x_\beta)+i(y-y_\beta)=r_{1\beta}e^{i\theta_{1\beta}}$$

$$z-\frac{a^2z_\beta}{|z_\beta|^2}=x-\frac{a^2x_\beta}{\mathfrak{L}_\beta^2}+i\left[y-\frac{a^2y_\beta}{\mathfrak{L}_\beta^2}\right]=r_{2\beta}e^{i\theta_{2\beta}}$$

such that when

$$|z|=a, r_{2\beta}=ar_{1\beta}/\mathfrak{L}_\beta \text{ and } \Psi=0$$

Then

$$\frac{dw}{dz}=-\tilde{u}^\circ+i\tilde{v}^\circ=e^{-i\theta}(-v^\circ+iu^\circ) \tag{9}$$

From the Bernoulli equation

$$-\Phi_{,t}+\frac{u^{\circ 2}+v^{\circ 2}}{2}+p/2=f(t) \tag{10}$$

the coefficient of pressure on the surface is

$$C_p=p-p_\infty=4\dot{a}\cos\theta-2\sum_\beta(\Gamma_\beta/2\pi)(\mathring{\theta}_{1\beta}-\mathring{\theta}_{2\beta})|_{r=a}-(u_\infty^{\circ 2}+v_\infty^{\circ 2})-\{2\frac{d}{dt}(a\dot{a})[\log a-\lim_{r\to\infty}\log r]-1\} \tag{11}$$

The bracketed term includes a logarithmic singularity. This is a reflection of the fact that the pressure waves emanating from the changing radius travel with an infinite propagation speed in incompressible flow, thus precluding a constant freestream pressure. This term is independent of θ, however, and does not contribute to drag. It must be considered an arbitrary additive constant in the pressure distribution and so the theory is confined to qualitative predictions of pressure distribution.

Boundary Layer

A finite difference solution is used for the boundary-layer region on an expanding-contracting cylinder. The solution technique entails the derivation of the pertinent boundary-layer equations and a transformation to a form of the equations such that the Hall method (Ref. 22) is applicable. The unsteady two-dimensional Navier-Stokes equations in polar coordinates are (nondimensionalizing as in the outer flow and with $\tau=2\tau^*/\rho U^2$)

$$DE\ \frac{(rv)_{,r}}{r}+\frac{u_{,\theta}}{r}=0$$

$$\frac{Du}{Dt}+\frac{uv}{r}=-\frac{p_{,\theta}}{2r}+\delta^2\left[L[u]+\frac{2v_{,\theta}}{r^2}\right] \tag{12a}$$

$$\frac{Dv}{Dt}-\frac{u^2}{r}=-\frac{p_{,r}}{2}+\delta^2\left[L[v]-\frac{2u_{,\theta}}{r}\right]$$

where $\frac{D}{Dt}=(\ )_{,t}+\frac{u(\ )_{,\theta}}{r}+v(\ )_{,r}$

$$L[\ ]=(\ )_{,rr}+\frac{(\ )_{,r}}{r}+\frac{(\ )}{r^2}+\frac{(\ )_{,\theta\theta}}{r^2}$$

$$IC\ t=t_0>0;\ u=f(r,\theta), v=g(r,\theta) \tag{12b}$$

and boundary conditions at the surface

$$BC\ r=a(t): u=0, v=\dot{a} \tag{12c}$$

Defining the inner variables

$$[\bar{u},\bar{v}]=[u,(v-a\dot{a}r)/\delta],[\bar{\theta},\bar{r},\bar{t}]=\left[\theta,\frac{r-a(t)}{\delta},t\right] \tag{13}$$

substituting into Eqs. (36), letting $\delta\to 0$, one obtains the (laminar) boundary-layer equations.

$$DE\ \frac{\bar{u}_{,\bar{\theta}}}{a}+\bar{v}_{,\bar{r}}=0$$

$$\bar{u}_{,\bar{t}}+\bar{v}\bar{u}_{,\bar{r}}+\frac{\bar{u}\bar{u}_{,\bar{\theta}}}{a}-\frac{\dot{a}\bar{r}\bar{u}_{,\bar{r}}}{a}+\frac{\dot{a}}{a}\bar{u}=-\frac{p_{,\bar{\theta}}}{2a}+\bar{u}_{,\bar{r}\bar{r}}$$

$$0=-p_{,\bar{r}},\ \omega=\frac{\bar{u}_{,\bar{r}}}{\delta},\ \tau=2\delta\bar{u}_{,\bar{r}} \tag{14a}$$

with

$$IC\ t=t_0: \bar{u}=f'(\bar{r},\bar{\theta}), \bar{v}=g'(\bar{r},\bar{\theta}) \tag{14b}$$

$$BC\ 1)\ \bar{r}=0: \bar{u}=\bar{v}=0$$

$$BC\ 2)\ \bar{r}\to\infty: \bar{u}\to u_\infty^\circ(\bar{\theta},\bar{t}) \tag{14c}$$

BC 2) being derived from the matching concept.

As such, the Hall scheme of integration is not applicable. If the transformation is made,

$$u^i=a\bar{u},\ v^i=\bar{v}-\frac{\dot{a}}{a}\bar{r} \tag{15}$$

then the problem is

$$DE\ \frac{u^i_{,\theta}}{a^2}+v^i_{,\bar{r}}=-\frac{\dot{a}}{a}$$

$$u^i_{,t}+\frac{u^iu^i_{,\bar{\theta}}}{a^2}+v^iu^i_{,\bar{r}}=(au_\infty^\circ)_{,t}+\frac{(au_\infty^\circ)_{,\bar{\theta}}}{a^2}+u^i_{,\bar{r}\bar{r}}$$

$$\omega=\frac{u^i_{,\bar{r}}}{a\delta},\ \tau=\frac{2\delta u^i_{,\bar{r}}}{a} \tag{16a}$$

$$IC\ t=t_0: u^i=f''(\bar{r},\bar{\theta}), v^i=g''(\bar{r},\bar{\theta}) \tag{16b}$$

$$BC\ 1)\ \bar{r}=0: u^i=v^i=0$$

$$BC\ 2)\ \bar{r}\to\infty: u^i\to au_\infty^\circ(\bar{\theta},t) \tag{16c}$$

where $p_{,\bar{\theta}}$ has been evaluated at $r\to\alpha$ by virtue of $p_{,r}=0$.

Except for the source term "$\dot{a}/a$" in the continuity equation and the factor "$1/a^2$" multiplying the $(\ )_{,\bar{\theta}}$ terms, the form of the equation is identical with the classical equations. Thus modifying the Hall method by the inclusion of a source term, modifying finite difference in $\bar{\theta}$ terms by the factor $1/a^2(t)$, and giving $u(r,0,t)=0$ at the stagnation point, the Hall scheme is applicable. (In the numerical integration, $\Delta r=0.14$, $\Delta t=0.125$, $1^\circ\le\Delta\theta\le 5^\circ$, were used).

Boundary-Layer Separation

The separation point was determined as the value of $\theta=\theta_{sk}$ one grid point upstream of the θ at which $\tau\le 0$. This is the steady-state criterion, used in lieu of a definitive criterion for unsteady flow.[23]

Vortex Birth

At each step, t_k, of numerical integration of the boundary layer, a point vortex of strength, Γ_β (and its images), labeled $\beta=k$ is born. The label β is then fixed for succeeding times. With the vortex flux at the separation point

$$\Gamma_{,t}(t_k)=\int_0^\infty \bar{u}_{,t}\bar{u}\,d\bar{u}=u_s^2/2 \tag{17}$$

by virtue of no-slip, where u is the instantaneous velocity profile in the boundary layer determining vortex flux,

$$\Gamma_\beta|_{\beta=k}=\Gamma_{,t}(t_k)\Delta t_k;\ u_s t_k=t_{k+1}-t_k \tag{18}$$

For the just born vortex to satyisfy no-slip, it is located at $[a+m_k, \theta_{sk}]$ where

$$m_k=|\Gamma_\beta|/\pi|u_s(\theta_{sk})|=|\tfrac{1}{2}u_s(\theta_{sk})|\Delta t_k/2\pi \tag{19}$$

where $|u_s(\theta_{sk})|$ is due to the outer flow minus the just born vortex.

Alternatively, if m_k is found from the first moment of the vorticity, Eq. (19) determines the Δt_k of the numerical integration. However this yields unnecessarily small values of Δt_k. For computation Δt_k was chosen such that the Hall scheme is workable and Eq. (19) yielded $m_k<0.1a$ (i.e., within the boundary layer).

Rear Shear Layer

The mathematical model described so far leaves the satisfaction of the no-slip condition at the rear of the cylinder in the absence of the boundary layer (i.e., where the separation point is upstream) to the velocity induced by the array of free shed point vortices. These induce a velocity on the surface counter to that given by uniform flow over a cylinder. However, the counter-velocity sometimes exceeds the latter velocity and the no-slip condition is not satisfied.

To account for the no-slip condition, a *rear shear layer* is introduced. The rear shear layer is similar to a boundary layer except that the outer flow is rotational. Since there is no theory for such a rear shear layer (time-dependent) and since its prime contribution is the production of vorticity, then it is postulated: a) there exists a rear shear layer when $|u_s|>0.1$; b) the separation point of rear shear layer is given as a function of the boundary-layer separation point location by means of the following:

$$\frac{\theta_s^f-\theta_m^f}{\theta_0-\theta_m^f}=\frac{\theta_m^r-\theta_s^r}{\theta_m^r-\theta_0} \tag{20}$$

Physically, this states that the rear shear layer can exist over the same fraction of a region of adverse pressure gradient without separation that the boundary layer could. Thus the location of the separation region of the rear shear layer is primarily a function of the boundary-layer separation location.

Point vortices are born from the rear shear layer as from the boundary layer [Eqs. (17-19)]. Now with this algorithm, the rear shear layer separation point may oscillate (as opposed to the monotonic behavior of the boundary-layer separation point). Thus a point vortex may be born at one instant but be recovered by the shear layer before it enters the outer flow. To take this behavior into account the condition was made that vortices are born only when the separation point is stationary or moving downstream. In addition, since the strengths are small, N point vortices are lumped together where $N\leq 5$ and the total strength ≤ 0.1.

Convection

Each point vortex is then convected by the outer flow such that

$$-\bar{z}_{\beta k+1}=-\bar{z}_{\beta k}+\Delta t_k\,dw/dz(z_{\beta k},t_k) \tag{21}$$

where $\bar{z}=x-iy$ and dw/dz is the complex velocity of the outer flow minus that due to the point vortex at $z_{\beta k}$.

Diffusion

For point vortices as given by inviscid theory the induced velocity distribution is $\Gamma/2\pi r$, $r>0$ and zero for $r=0$, where r is the distance from the point vortex. Such a velocity distribution could induce local high velocities for small r as when a point vortex lies close to the surface or two point vortices are close. While such peaks have been found experimentally, their small scale is incompatible with this mathematical model (particularly with the approximation employed in convection). To remove such behavior, diffusive effects are taken into consideration in the following way: following Ref. 24, consider a stationary isolated vortex born at $t=0$ as a point vortex in a viscous fluid. Its induced velocity field is

$$u(r,t)=(\Gamma_0/2\pi r)[1-\exp(-Re_{2DUS}r^2/4t)] \tag{22}$$

where Γ_0 is its initial strength. This has a maximum at $r=r_c(t)$ where

$$r_c(t)=(5.04tRe_{2DUS})^{1/2} \tag{23}$$

such that for $r>r_c$, the velocity distribution for an inviscid point vortex of constant strength is closely approximated. To minimize computation time, inviscid point vortices of constant strength are employed with induced velocity distributions of

$$u=0;r<r_c=\Gamma/2\pi r;r>r_c \tag{24}$$

with $r_c=0.05$, an average value for values of Re_{2DUS} used in the applications. Such an approach is compatible with the convection approximation which entails errors of $0[(\Delta t^2)]$ in the displacement.

The cut-off radius is applied as follows: in the velocity expressions obtained from Eqs. (18) and (9), $r_{1\beta}$ and $r_{2\beta}$ occur in the denominator. Then r_c *is used as, with* $i=1, 2$

$$r_{i\beta}=\infty;r_{i\beta}<r_c,=r_{i\beta};r_{i\beta}\geq r_c \tag{25}$$

Coalescence

Since the number of point vortices grows with time with consequent increase in computation time, the number of vortices is reduced at certain times by means of coalescing pairs of vortices into one vortex. The strength of the new vortex is the algebraic sum of the strengths of the coalesced vortices and its position is the arithmetic average, weighted by absolute strengths, of the coalesced vortices.

Stability

It is known that symmetric arrays of point vortices are unstable and that a perturbation is required in the symmetrical array such that a stable asymmetric array can be attained. A number of runs were made for cylinders of constant radius and time-varying radius with perturbations inserted at early times and it was observed that the model is capable of yielding realistic asymmetric wakes. However, the degree of asymmetry grows slowly with time such that for the particular applications of the theory in this work, in which angles of attack and fineness ratios were moderate, the assumption of symmetric wakes was made.

This places a limitation on the angle of attack and fineness ratio for the application of the theory as is. However, the inclusion of asymmetric wakes is easily accomplished but with consequent increase in computer cost. The theory in this ex-

tended state would then be applicable to larger angles of attack and fineness ratios[6] but there is an upper bound to such generalizations since the direct use of the cross-flow analogy cannot be extended to the case of a three dimensional body traveling at constant speed but with a time-varying wake, a four-dimensional problem.

Drag

At representative times, the drag is computed in Eq. (4). The pressure is obtained from the Bernoulli equation, Eq. (11) and the shear stress from the boundary-layer solution $\tau = 2\delta\bar{u}, _{\bar{r}} = 2\delta\bar{u}(\Delta\bar{r},\theta,t)/\Delta\bar{r}$ by virtue of the no-slip condition.

Within a completely inviscid model and a fixed geometry, the drag may be obtained using the vortex-impulse concept or Lagally's theorem. However, drag is obtained herein by pressure and shear integration since the wake model, while primarily inviscid, does have diffusive effects and, more importantly, the surface pressures are of interest in establishing the equivalence property. Computational times are of the same order.

Results and Discussion

The theory has been applied to an ellipsoid of revolution, an ogive-cylinder, and, to a lesser extent, to a Haack-Adams body. The case of the ellipsoid of revolution will be dealt with at length (for ogive-cylinder results, see Refs. 25 and 26) since this presents a severe test because the geometry is that of a closed-ended body such that for all angles of attack, there may not exist any unseparated boundary layer on the aft end even on the windward meridian. The theory as presented so far does not cover this eventuality (although it may easily be extended). However, even without this specific capability, meaningful results can be obtained. Also, inviscid theory yields $C_N = 0$.

In Ref. 27, the pressure distribution, normal forces, and moments for an ellipsoid of revolution of fineness ratio $f = 4$ were obtained at Mach number <0.1 and $Re_{3DS} = 4.97\text{x}10^5$ over an angle-of-attack range $0 < \alpha < 20°$. No information on the state of the boundary layer was given. The maximum $Re_{2DUS} = 16.5 \times 10^3$ at $\alpha = 20°$. The $\tilde{a}$ chosen was taken to be $(1/\mathcal{L}) \int_0^{\mathcal{L}} r_0^*(z^*)\, d\hat{z}^*$, an average radius.

The basic result for the ellipsoid, the comparison of the values obtained by this technique and inviscid theory with experimental data for the normal force and pitching moment about the midpoint are presented in Fig. 2. In this case the improvement of this technique over inviscid theory ($C_N = 0$) is marked.

The curves of Fig. 2 are a result of the integration of the section normal force coefficient $c_n(\hat{z}\,\alpha)$ over $\hat{z}$. One integrand, $c_n(\hat{z},\alpha)$is presented in Fig. 3 as a function of the axial station$\hat{z}$ at $\alpha = 20°$. Interpreting these curves as integrands, attention has to be paid to the behavior in the neighborhood of the base. In this region, there is no boundary layer; the tail lies within the wake. As noted earlier the theory as developed thus far does not handle this situation although the extension can easily be made. And before the computations reach the section of no boundary layer, the radius *a(t)* may change rapidly (for such a closed-ended body as the ellipsoid) such that very fine integration meshes are required with consequent increase in computer time. Furthermore, the basic assumptions of the two-dimensional unsteady boundary-layer solution technique may fail, particularly with regard to the property of no pressure change across the boundary-layer and longitudinal effects would enter.

In lieu of increasing the complexity of the technique, computation was formally stopped at $\hat{z} = 0.9 \equiv \hat{z}_f$ and a straight line drawn to complete the curve at $(c_n, \hat{z}) = (0, 1.0)$, a theoretically exact point. Fig. 3 shows the differences in behavior for two stopping stations $\hat{z}_f = 0.9$ and 1.0. The latter value, in both cases, departs from the experimental data.

Figure 4 depicts the regions of separation of a three dimen-

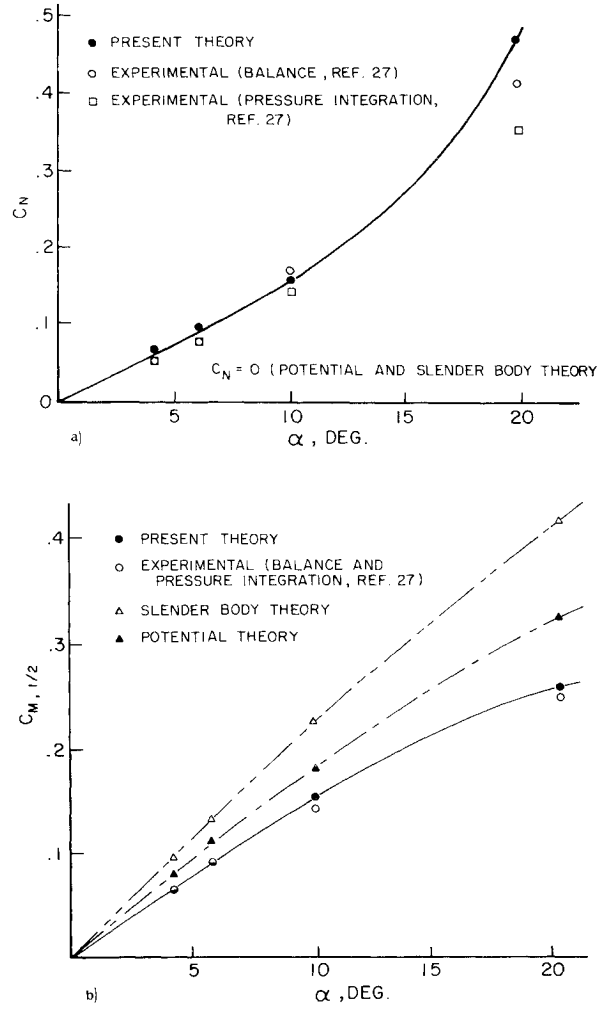

Fig. 2a) Normal force on ellipsoid as a function of angle of attack. b) Pitching moment on ellipsoid as a function.

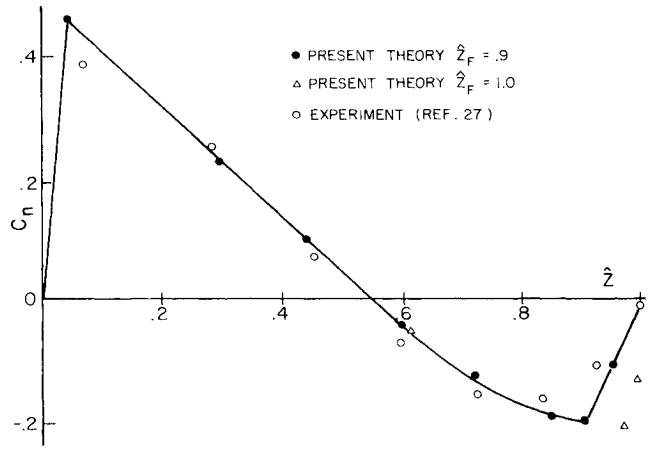

Fig. 3 Normal force distribution on ellipsoid, $\alpha = 20°$.

sional steady flowfield as determined by this theory compared with that determined by a finite difference solution.[28] The agreement is fairly good. Of note are the divergences on the aft windward region but in this region, the particular behavior determined by means of this technique agrees with experimental data.[29] These results may be fortuitous since the implication is that the separation of a three dimensional (probably) turbulent boundary layer is describable by a two-dimensional unsteady laminar boundary layer, as discussed

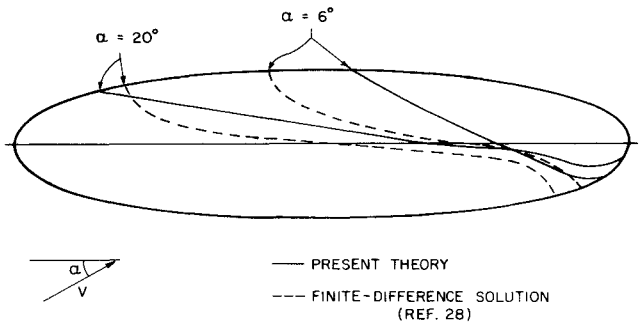

Fig. 4 Theoretical separation regions over ellipsoid.

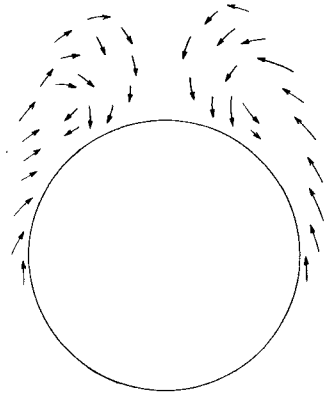

Fig. 5 Cross wake pattern on ellipsoid, $\hat{z}=0.863$, $\alpha=20°$.

earlier. No attempt was made to compute other boundary-layer properties such as thickness.

Figure 5 shows the cross wake vortex pattern at $\hat{z}=0.863$ and $\alpha=20°$ in terms of a set of directed line segments. The position of a point vortex at that axial station or time is given by the foot of the line segment and its position at the succeeding axial station or time is given by the head of the line segment. Thus the distribution of vorticity is indicated (only by the presence or absence of vorticity) and since the point vortices are convected with the flow, a partial stream line pattern is given.

The ogive-cylinder application[30] was for a Mach number = 0.3 and $0<\alpha<24$. For this case, theoretical and experimental data[30] (also obtained at Purdue University) agreed if a 40% reduction in wake vortex strength was imposed.[6] This is believed to be due to the geometrical end conditon. Thus, it is recommended that for furture applications, vortex strengths be multiplied by a factor, σ, given by

$$\sigma=1.0\text{-}0.8r_o(\ell)/d \qquad (26)$$

(a linear fit over the two test cases).

In addition, a Haack-Adams body with Mach numbers 1.5 and 3.97 over a small α-range, $0<\alpha<10°$ was treated.[31] (These runs were performed by E. J. Landrum at NASA-Langley.) Partial success was achieved at the lower Mach number (and $\sigma=1$, reflecting wave drag) but theoretical values were low at the higher Mach number.

As a result of these test cases, it is recommended that application of this theory, with asymmetric wake capability, be limited to angles of attack less than 40° and Mach numbers (freestream, not cross flow) less than 0.8.[6] However, fuller substantiation of this recommendation would require further testing, particularly regarding the wake vortex strength reduction factor.

Computation Times

The time for computing the forces and moments on an ellipsoid of revolution at an angle of attack of 20° on a CDC 6500 at Purdue University was 15.7 minutes. Since the time is proportional to $(df/\hat{a})\tan\alpha=2f\tan\alpha$, approximate times for other bodies and angles of attack can be found. It is believed that substantial reductions in computational times can be made particularly in the area of wake modeling. However, at the present stage, the times are well below those of finite difference solutions.

Conclusions

A method has been developed to determine the forces and moment on a body of revolution in separated flow. The method requires no a priori knowledge of the flowfield. (Although the method used in the test cases assumed symmetric wakes, extension to asymmetric wakes is easily accomplished.) One empirical factor, a function of body geometry, Eq. (26), was used. Results for the forces, moments, and separation regions compare well with experimental data for moderate angles-of-attack $\alpha<25°$, moderate fineness ratios $f<11$; low Mach numbers, and moderate cross-flow Reynolds numbers, $Re_{2DUS}<10^5$.

The problem approached by the present theory is a complex one. To categorize all the pertinent flow phenomena is a difficult task, particularly since experimentation may introduce new parameters (e.g., scale effect). Possibly the best attempt in this direction is that of Ref. 6 and in the context of that survey and the results obtained it is recommended that further testing and applications of the theory, with Eq. (26) and extended to the asymmetric wake capability, be confined to $\alpha<40°$, $f<12$, Mach numbers <0.8, and cross-flow Reynolds numbers, $Re_{2DUS}<10^5$.

In the context of this theory employing the cross flow analogy directly with no a priori flowfield properties required, it has been seen that the analogy is relevant but not sufficient. Thus, the unsteady cross-flow analogy is deemed a worthwhile approach to a complex problem, aided by efficient use of the computer. In addition there is the potential of such solutions, to bring about further physical understanding of the flow phenomena with consequent new analytic solutions.

References

[1]Holt, A., ed., *Proceedings of 2nd International Conference on Numerical Methods in Fluid Dynamics,* Springer-Verlag, Berlin, 1971.

[2]*Proceedings: AIAA Computational Fluid Dynamics Conference,* Palm Springs, Calif., July 1973.

[3]Thwaites, B., ed., *Incompressible Aerodynamics,* Oxford, 1960, 409ff.

[4]Kuchemann, D. and Weber, J., "Vortex Motions," *Zeitschrift für Angewandte Mathmatik und Mechanik,* Vol. 45, Dec. 1965, pp. 457-474.

[5]Wang, K. C., "Zones of Influence and Dependence for Three Dimensional Boundary Layer Equations," *Journal of Fluid Mechanics,* Vol. 48, Part 2, July 1971, pp. 397-404.

[6]Thompson, K. D., "The Estimation of Viscous Normal Force, Pitching Moment, Side Force and Yawing Moment on Bodies of Revolution of Incidences Up to 90°," WRE-Rep.-782 (WR&D), Australian Defense Scientific Service, Melbourne, Aus., Oct. 1972.

[7]Allen, H. J. and Perkins, E. W., "A Study of Effects of Viscosity on Flow Over Slender Inclined Body of Revolution," Rept. 1048, 1951, NASA

[8]Jorgensen, L. H. and Perkins, E. W., "Investigation of Some Wake Vortex Characteristics of an Inclined Ogive-Cylinder Body at M=2," Rept. 1371, 1958, NASA.

[9]Bryson, A. E., "Symmetric Vortex Separation on Circular Cylinders and Cones," *Journal of Applied Mechanics,* Vol. 26, Dec. 1959, pp. 643-648.

[10]Sarpkaya, T., "An Analytical Study of Separated Flow About Circular Cylinder," *Journal of Basic Engineering,* Vol. 90, Dec. 1968, pp. 511-520.

[11]Walitt, L., Trulio, J. G., and King, L. S., *A Numerical Method of*

Computing Three-Dimensional Viscous Supersonic Flow Fields About Slender Bodies, SP-228, 1969, pp. 265-322, NASA.

[12]Schindel, L., "Effects of Vortex Separation on Lift Distribution of Elliptic Cross Section," *Journal of Aircraft,* Vol. 6, No. 6, Nov.-Dec. 1969, pp. 537-543.

[13]Kelly, H., "Estimate of Normal Force and Pitching Moment for Blunt Based Body of Revolution," Vol. 21, No. 8, Aug. 1954, pp. 549-555, 565.

[14]Angelucci, S. B., "A Multivortex Method for Axisymmetric Bodies at Angle of Attack," *Journal of Aircraft,* Vol. 8, No. 12, Dec. 1971, pp. 959-966.

[15]Mello, J. F., "Investigation of Normal Force Distribution and Wake Vortex Characteristics of Body of Revolution at Supersonic Speeds," *Journal of the Aerospace Sciences,* Vol. 26, No. 3, March 1959, pp. 155-168.

[16]Jorgensen, L. H., "Estimation of Aerodynamics for Slender Bodies Alone and With Lifting Surfaces at $\beta = 0$ to 90,°" *AIAA Journal,* Vol. 11, No. 3, March 1973, pp. 409-412.

[17]Thompson, K. D. and Morrison, D. F., "The Spacing Position and Strength of Vortices in the Wake of Slender Cylindrical Bodies at Large Incidence," *Journal of Fluid Mechanics,* Vol. 50, Pt. 4, Dec. 1971, pp. 751-783.

[18]Marshall, F. J., "Impulsive Motion of a Cylinder and Viscous Cross Flow," *Journal of Aircraft,* Vol. 7, No. 4, July-Aug. 1970, pp. 371-373.

[19]Morkovin, M., "Flow Around Circular Cylinder—a Kaleidoscope of Challenging Fluid Phenomena," ASME Symposium on Fully Separated Flows, Philadelphia, Pa., May 1964.

[20]Thoman, D. C. and Szewczyk, A. A., "Time Dependent Viscous Flow Over a Circular Cylinder," *Physics of Fluids,* Suppl. II, 1969, pp. II-76-II80.

[21]Wundt, H. "Wach stum der laminaren Grenzschicht an schräg ange stromten Zylinder bei Anfahrt aus der Ruhe," *Ingenieur-Archivum,* Vol. 23, 1955, pp 212-230.

[22]Hall, M. G., "A Numerical Method for Calculating the Unsteady Two Dimensional Laminar Boundary Layer," *Ingenieur-Archivum,* Vol. 38, 1969, pp. 97-106.

[23]Marshall, F. J., ed., *Fluid Dynamics of Unsteady, Three Dimensional and Separated Flows,* Proceedings of Project Squid Workshop, June 1971. (Available from Project Squid Headquarters, Purdue University).

[24]Schaefer, J. W. and Eskinazi, S., "The Vortex Street Generated in a Viscous Fluid," *Journal of Mechanics,* Vol. 6, Pt. 2, Aug. 1959, pp. 241-260.

[25]Marshall, F. J. and Deffenbaugh, F. D., "Separated Flow Over Bodies of Revolution Using an Unsteady Discrete-Vorticity Cross Wake. Part 1—Theory and Applications," CR-2415, June 1974, NASA.

[26]Marshall, F. J. and Deffenbaugh, F. D., "Separated Flow Over Bodies of Revolution Using an Unsteady Discrete-Vorticity Cross Wake. Part II—Computer Program Description," CR-2415, June 1974, NASA.

[27]Jones, R., "Distribution of Normal Pressures on Prolate Spheroid," R&M 1061, 1925, Aeronautical Research Council, London.

[28]Wang, K. C., "Three Dimensional Boundary Layer Near Plane of Symmetry of a Spheroid of Incidence," *Journal of Fluid Mechanics,* Vol. 43, Pt. 1, Aug. 1970, pp. 187-209.

[29]Eichelbrenner, E. A. and Oudart, A., "Methode de Calcul de la Couche Limite Tridimensionelle Application a un Corps Fuselle Incline Sur le Vent," ONERA Publication No. 76, 1955.

[30]Tinling, B. E. and Allen, C. Q., "An Investigation of the Normal Force and Vortex Wake Characteristics of an Ogive-Cylinder Body at Subsonic Speeds," TN D-1297, April 1962, NACA.

[31]Unpublished data, NASA Langley Research Center, Hampton, Va.